doi: 10.3969/j.issn.0490-6756.2017.06.018

高压下 LaB_6 的弹性和热力学性质的第一性原理计算

何　熹[1,2], 傅　敏[2], 于白茹[1]
(1. 四川大学物理科学与技术学院, 成都 610064;2. 四川大学原子与分子物理研究所, 成都 610065)

摘　要: 运用平面波赝势密度泛函理论,研究了 CsCl 结构的 LaB_6 在高压下的弹性和热力学性质. 计算中使用了广义梯度近似,得到在零温零压下 LaB_6 的晶格常数和已知的实验及其它理论结果相符. 同时,我们还得到了 LaB_6 的弹性常数 C_{ij},体弹模量 B,剪切模量 G,杨氏模量 E,德拜温度 Θ_E,泊松系数 σ,压缩波速 V_L 和剪切波速 V_S 与压强的关系. 计算发现 LaB_6 在压强低于 14 GPa 时具有力学稳定性. 根据准谐德拜模型,我们还预测了 CsCl 结构 LaB_6 的热力学性质,对 0～14 GPa 和 0～1500 K 范围内热膨胀系数和比热容的变化进行了研究. 最后分析了 LaB_6 在零温零压和高压下的电子态密度图.

关键词: 密度泛函理论; 弹性性质; 电子性质; 热力学性质
中图分类号: O521+.2　　**文献标识码**: A　　**文章编号**: 0490-6756(2017)06-1239-11

Elastic and thermodynamic properties of LaB_6 under pressure: a first-principles study

HE Xi[1,2], *FU Min*[2], *YU Bai-Ru*[1]
(1. College of Physical Science and Technology, Sichuan University, Chengdu 610064, China;
2. Institute of Atomic and Molecular Physics, Sichuan University, Chengdu 610065, China)

Abstract: The elastic and thermodynamic properties of CsCl-type structure LaB_6 under high pressure are investigated by first-principles calculations based on plane-wave pseudopotential density functional theory method within the generalized gradient approximation (GGA). The calculated lattice parameters of LaB_6 under zero pressure and zero temperature are in good agreement with the existing experimental data and other theoretical data. The pressure dependences of the elastic constants, bulk modulus B (GPa), shear modulus G, Young's modulus E, elastic Debye temperature Θ_E, Poisson ratio σ, compressional wave velocity V_L and shear wave velocity V_S are also presented. An analysis for the calculated elastic constants has been made to reveal the mechanical stability of LaB_6 up to 14 GPa. The thermodynamic properties of the CsCl-type structure LaB_6 are predicted using the quasi-harmonic Debye model. The variations of thermal expansion coefficient α and the specific heat capacity C_v are obtained systematically in the ranges of 0～14 GPa and 0～1500 K. At last, the pressure dependences of the density of states are also investigated.

Keywords: Density functional theory; Elastic properties; Electronic properties; Thermodynamic properties

收稿日期: 2017-10-19
基金项目: 国家自然科学基金(11204192)
作者简介: 何熹(1992－),男,主要研究领域是第一性原理计算.
通讯作者: 于白茹. E-mail: yubrscu@126.com

1 Introduction

The rare-earth hexaborides RB_6 have attracted extensive experimental and theoretical interest due to their intriguing physical properties. For example, CeB_6 is a dense Kondo compound and has interesting low-temperature magnetic phases[1]. SmB_6 is also an exemplary Kondo insulator which features an energy gap in the electronic density of states (DOS) whose magnitude is strongly temperature dependent and only fully developed at low temperatures[2]. EuB_6 is a ferromagnetic semiconductor with a transition temperature $T_C = 15$ K. Below T_C the electrical resistivity is drastically reduced, above T_C a very large negative magnetoresistance is observed[3]. Among these compounds, lanthanum hexaboride (LaB_6) has a special place. LaB_6, which is metallic at room temperature and becomes a superconductor at $T_C = 0.45$ K[4, 5], is a hard, refractory and stable material owing to strong B-B covalent bonds[6]. And it is a thermionic electron emitter with a low work function, high brightness and long life compared with conventional tungsten filaments[7].

The structural, elastic, and thermodynamic properties of LaB_6 have been investigated experimentally and theoretically by several groups. Early in 1977, Tanaka *et al.*[6] studied the elastic constants of LaB_6 for the first time by the measurements of the transit time of pules of longitudinal and transverse ultrasonic wave propagating in single crystal. An early electronic structure calculation was estimated by Kubo *et al.*[8], using the three-dimensional Lock-Crisp-West (LCW) folded momentum densities (3D LCW FMD's) within local-density approximation (LDA) method. It's indicated that the Fermi surface topology plays an important role in the determination of structures. Mandrus *et al.*[9] explained the temperature dependence of the specific heat and resistivity of LaB_6 well by using a model of La ions as independent Einstein oscillators embedded in a Debye framework of boron ions. Xu *et al.*[10] investigated the elastic and thermal properties of LaB_6 in the framework of density-functional theory (DFT) with a quasi-harmonic Debye model. Bai *et al.*[11] achieved the structure and chemical bond characteristics of LaB_6 by means of the density functional theory using the state-of-the-art full-potential linearized augmented plane wave (FPLAPW) method. In addition, Gürel *et al.*[12] performed an ab initio study of structural, elastic, lattice-dynamical, and thermodynamic properties of rare-earth hexaborides LaB_6 within the density functional theory and linear-response formalism using pseudopotentials and a plane-wave basis. There have been many other works to investigate the LaB_6 crystal and its properties[13, 14].

What attracts us most is the pressure induced phase transition of LaB_6, which has recently provoked a great deal of controversy. By using the Raman and angle dispersive X-ray diffraction (ADXRD), Teredesai *et al.*[15] proposed that the pressure induced structural phase transition from CsCl-type structure to the orthorhombic structure occurs at around 10 GPa. While Godwal *et al.*[16] also using the Raman and ADXRD, proposed that there is no structural or electronic phase transition up to at least 25 GPa in CsCl-type structure.

The most common assessment of mechanical properties can be made by the determination of its elastic constants. Especially, the elastic constants of materials at high pressure are essential in order to predict and understand material response, strength, mechanical stability, and phase transition. The comprehensive analysis of elastic constants can provide a deeper insight into the hardness of materials. Furthermore, elastic properties are also related thermodynamically to the specific heat, thermal expansion, Debye temperature, melting point, and so on. Thus in this work, we put our investigation emphases mainly on the elastic and thermodynamic properties of CsCl-type structure LaB_6(space group $Pm\bar{3}m$) under pressure. From the calculated elastic constants, we will study its mechanical stabilities and anisotropic behaviors, as well as the bulk modulus, shear

modulus, Young's modulus, Poisson's ratio, elastic Debye temperature of LaB_6 at diverse pressures. Because the mechanical properties of this substance are studied in detail for the first time, we hope that our work can provide useful help for future research in both experimental and theoretical studies. The rest of the paper is organized as follows.

The theoretical method is introduced and the computation details are given in Section 2. Some results and discussion are presented in Section 3. Finally, the summary of our main results and conclusions are given in Section 4.

2 Theoretical method and calculation details

2.1 Total energy electronic structure calculations

In the electronic structure calculations, we employ the plane-wave pseudopotential density functional theory method[17] through the Cambridge Serial Total Energy Package (CASTEP)[18] code together with both the generalized gradient approximation (GGA) proposed by Perdew *et al*.[19] and the local density approximation (LDA) proposed by Vosko *et al*.[20] for exchange-correlation potentials. A plane-wave basis set with energy cut-off 390 eV is applied. Pseudo-atom calculations are performed for La $5d^16s^2$ and B $2s^22p$. For the Brillouin-zone sampling, we use the $6\times6\times6$ Monkhorst-Pack mesh[21], where the self-consistent convergence of the total energy is at 5.0×10^{-7} eV/atom. The tolerance for geometry optimization is set to within 5.0×10^{-6} eV/atom, the maximum ionic force within 0.01 eV/Å, the maximum ionic displacement within 5.0×10^{-4} Å, and the maximum stress within 0.02 GPa. The tolerance for elastic constants is set to within 1.0×10^{-6} eV/atom, the maximum force within 0.0002 eV/Å, and the maximum strain amplitude within 0.003 GPa. These parameters are carefully tested. It is found that these parameters are sufficient to lead to a well-converged total energy.

2.2 Elastic properties

To calculate the elastic constants under hydrostatic pressure p, we use the symmetry-dependent strains that are non-volume conserving. The elastic constants, C_{ijkl}, with respect to the finite strain variables are defined as[22]

$$C_{ijkl}=\left(\frac{\partial\sigma_{ij}(x)}{\partial e_{kl}}\right)_x \tag{1}$$

where σ_{ij} and e_{kl} are the applied stress and Eulerian strain tensors, and X, x are the coordinates before and after deformation, respectively. Under the hydrostatic pressure p, we have

$$C_{ijkl}=C_{ijkl}+\frac{p}{2}(2\delta_{ij}\delta_{kl}-\delta_{il}\delta_{jk}-\delta_{ik}\delta_{jl}) \tag{2}$$

where C_{ijkl} denote the second-order derivatives with respect to the infinitesimal strain (Eulerian), δ is the finite strain variable. The fourth-rank tensor C generally greatly reduces when taking into account the symmetry of the crystal. In a cubic crystal, it is reduced to three components, *i.e.* C_{11}, C_{12}, and C_{44}.

The bulk modules B and the shear modules G of the LaB_6 are taken as[23]

$$B=(B_R+B_V)/2 \tag{3}$$

$$G=(G_R+G_V)/2 \tag{4}$$

where R and V represent Reuss and Voigt boundaries, respectively.

$$B_V=B_R=(C_{11}+2C_{12})/3 \tag{5}$$

$$G_V=(C_{11}-C_{12}+3C_{44})/3 \tag{6}$$

$$G_R=5(C_{11}-C_{12})C_{44}/[4C_{44}+3(C_{11}-C_{12})] \tag{7}$$

The polycrystalline Young's modulus E and the Poisson's ratio σ are then calculated from these elastic constants using the following relations[24].

$$E=\frac{9BG}{3B+G} \tag{8}$$

$$\sigma=\frac{3B-2G}{2(3B+G)} \tag{9}$$

The elastic Debye temperature Θ_E may be estimated from the average sound velocity V_m[25]

$$\Theta_E=\frac{h}{k}\left[\frac{3n}{4\pi}\left(\frac{N_A\rho}{M}\right)\right]^{1/3}V_m \tag{10}$$

where h is Planck's constants, k Boltzmann's

constant, N_A Avogadro's number, n the number of atoms per formula unit, M the molecular mass per formula unit, ρ the density, and V_m is obtained from[25]

$$V_m = [\frac{1}{3}(\frac{2}{V_S^3} + \frac{1}{V_L^3})]^{-1/3} \quad (11)$$

where V_S and V_L are the shear and longitudinal sound velocities, respectively. The probable values of the average shear and longitudinal sound velocities can be calculated by[26]

$$V_S = \sqrt{\frac{G}{\rho}},\ V_L = \sqrt{\frac{B + (4/3)G}{\rho}} \quad (12)$$

2.3 Thermal properties

To investigate the thermal properties, we change the cell volume to obtain the corresponding energy, and then export them into the quasi-harmonic Debye model[27] to calculate the thermal properties. In this model, the non-equilibrium Gibbs function $G(V; p, T)$ has the following from:

$$G^*(V;p,T) = E(V) + pV + A_{vib}(\Theta(V);T) \quad (13)$$

where $E(V)$ is the total energy as a function of the call volume V, p is the hydrostatic pressure, $\Theta(V)$ is the Debye temperature as a function of V, and A_{vib} is the vibrational Helmholtz free energy.

Based on this model, the specific heat C_v, C_p, and the thermal expansion coefficient α can be deduced from the following expressions:

$$C_v = 3nk\left[4D(\Theta/T) - \frac{3\Theta/T}{e^{\Theta/T} - 1}\right] \quad (14)$$

$$\alpha = \frac{\gamma C_v}{B_T V} \quad (15)$$

where B_T is the static bulk modulus, γ is the Grüneisen parameter. They can be derived from $B_T(p,T) = V\left(\frac{\partial^2 G^*(V;p,T)}{\partial^2 V}\right)_{p,T}$ and $\gamma = -d\ln\Theta(V)/d\ln V$, respectively.

Through the quasi-harmonic Debye model, one could obtain the thermodynamic quantities of LaB_6 under pressure and high temperature. By applying the method, we have investigated the thermodynamic properties of several materials successfully[28-32].

3 Results and discussion

3.1 Structural properties

To investigate the elastic and thermodynamic properties, we must determine the structures of LaB_6 at first. LaB_6 has a bcc-like structure (space group $Pm\bar{3}m$) with La at the position (0, 0, 0) and B at the position (0.5, 0.5, x), where x is the positional parameter of the B atoms. The structure information can be absolutely described by lattice parameter a and positional parameter x. To determine the ground state structure of LaB_6, we use the following steps. Firstly, we fix the lattice parameter a and take a series of different values of positional parameters x to calculate the total energies E, so that we can obtain an $E-x$ curve and find a lowest energy E_{min}. The positional parameter x with the energy E_{min} is what we require. Secondly, with the obtained positional parameter x, we take a series of different values of lattice parameter a and repeat the above steps, the lattice parameter a also can be obtained. And for each a, we can calculate its corresponding primitive cell volume V, and then obtained the energy-volume ($E-V$) curve of LaB_6.

By fitting the calculated $E-V$ data to the third-order Birch-Murnaghan equation of state (EOS)[33], the bulk modulus B_0 at $p=0$ and $T=0$ can be obtained. All the equilibrium structure parameters and bulk moduli are listed in Tab. 1. It can be seen that our results of lattice parameter a, positional parameter x and bulk modulus B_0 from GGA calculations are well consistent with the experimental data[34, 35] and other theoretical data[11, 14]. And the errors of lattice parameter a are less than 0.1%, respectively. On the other hand, our LDA results are not satisfactory, which are a little small when compared with the experimental[34] and other theoretical data[11], except for bulk modulus B_0. Therefore, in this work, the GGA functional forms are applied in the following calculations.

Tab. 1　Calculated equilibrium lattice parameters of LaB_6, together with the experiment data and other theoretical results

	a /Å	x	B_0/GPa	B_0'
Present GGA (PBESOL)	4.151	0.1995	181.15	3.68
Present LDA (CA-PZ)	4.140	0.1991	179.97	3.76
Cal. [a]	4.1277	0.1997	180	3.79
Cal. [b]	4.1605	0.2009	182.4	
Cal. [c]	4.1557	0.1998	173.6	3.72
Exp. [d]	4.1568		172.0	
Exp. [e]	4.1569	0.1996		

[a] Calculated through Linear-response theory within LDA[12]; [b] Calculated through PW-PP method within GGA(RPBE)[11]; [c] Calculated through PAW method within GGA(PBE)[14]; [d] Measured by X-Ray diffraction measurements[35]; [e] Measured by PLD and XRD measurements[34].

The pressure and temperature dependence of the relative volume V/V_0 of LaB_6 are illustrated in Fig. 1. It is shown that, as the applied pressure increases from 0 to 14 GPa, the volume of LaB_6 decrease linear at the giving temperature, and the relative volume V/V_0 of higher temperature is less than that of lower temperature at the same pressure. This means, under higher temperature, LaB_6 is easier to be compressed, as temperature could make LaB_6 soft.

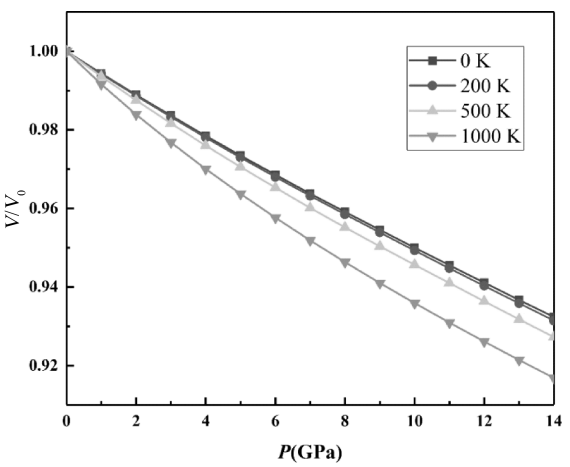

Fig. 1　Normalized primitive unit cell volume V/V_0 as a function of pressure

3.2　Elastic properties

We list our calculated elastic constants and aggregate elastic modulus B of the cubic structure LaB_6 at 0 K and 0 GPa in Tab. 2. It can be seen clearly that our results are in agreement with the other theoretical[12, 14] and experimental data[36], which indicates that our results are reasonable. In addition, from the Eq. (3), the bulk modulus B (in Tab. 2) obtained by our elastic constants is 177.9 GPa, which is consistent with the value estimated by fitting the $E-V$ data mentioned above.

Tab. 2　Calculated elastic constants C_{ij} of LaB_6 at 0 K and 0 GPa, in comparison with the experimental data and other theoretical results

	C_{11}/GPa	C_{44}/GPa	C_{12}/GPa	B/GPa
Present	460.6	94.0	36.6	177.9
Cal. [a]	466	88	37	180
Cal. [b]	473	92	24	173.6
Exp. [c]	463	89	45	184

[a] Calculated through Linear-response theory within LDA[12]; [b] Calculated through PAW method within GGA(PBE)[14]; [c] Measured by X-Ray diffraction measurements[36].

The pressure dependences of the elastic constants (C_{11}, C_{12} and C_{44}) of LaB_6 under pressure up to 14 GPa are summarized in Tab. 3. Unfortunately, to our knowledge, no experimental and theoretical data of the elastic constants are available to compare with our results in high pressure. The elastic constant C_{11} represents the elasticity in length, while C_{12} and C_{44} are related to the elasticity in shape. We find that all three elastic constants increase almost linearly with the increasing pressure which also can be observed from Fig. 2. Among them, C_{11} is more sensitive to pressure than C_{12} and C_{44}. For a cubic crystal, the mechanical stability leads to restrictions on the elastic constants under isotropic pressure as follows[37]: $\widetilde{C}_{44} > 0, \widetilde{C}_{11} > |\widetilde{C}_{12}|, \widetilde{C}_{11} + 2\widetilde{C}_{12} > 0$, where $\widetilde{C}_{ii} = C_{ii} - p\,(i = 1, 4), \widetilde{C}_{12} = C_{12} + p$. It is obvious from Tab. 3 that the elastic constants of LaB_6 satisfy all of these conditions at pressure up to 14 GPa. It is known that being a fourth-rank tensor property, elasticity is anisotropic for a cubic crystal, and it is conveniently expressed by the dimensionless parameter $A = 2C_{44}/(C_{11} - C_{12})$. For

isotropic elasticity, double C_{44} are equal to (C_{11} - C_{12}), thus $A=1$. Through the calculated elastic constants, one can obtain the Zener's anisotropy parameter A at different pressures and 0 K, which is also presented in Tab. 3. Our calculated A being 0.443 at 0 GPa and 0 K is in agreement with the value obtained by Duan *et al.*[14] ($A=0.42$ at 0 GPa and 0 K). It is showed that the Zener's anisotropy parameter A almost doesn't change with the elevated pressure p at 0 K, indicating that A deviates from 1 and the anisotropy of the cubic structure LaB_6 almost keeps stable in the processes of increasing pressure.

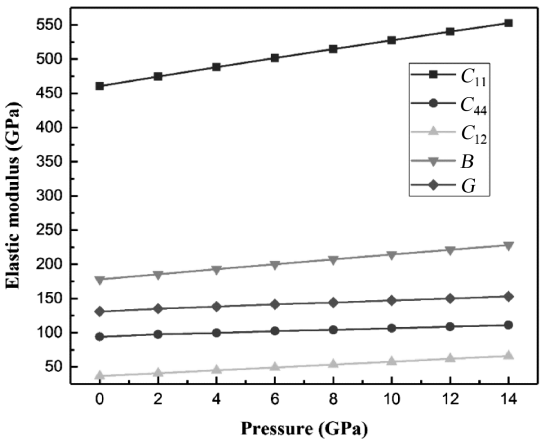

Fig. 2 Pressure dependencies of elastic constants of LaB_6 at 0 K

Tab. 3 Calculated elastic constants C_{ij} (GPa), bulk modulus B (GPa), shear modulus G (GPa), B/G, acoustic velocities, and V_L and V_S (km/s), and elastic Debye temperature Θ_E (K) of LaB_6 under pressure p (GPa)

p	0	2	4	6	8	10	12	14
C_{11}	460.6	474.4	488.3	501.6	514.8	527.6	540.2	552.6
C_{44}	94.0	97.5	99.6	102.3	104.1	106.4	108.8	111.0
C_{12}	36.6	40.7	45.0	49.2	53.4	57.6	61.7	65.9
B	177.9	185.3	192.8	200.0	207.2	214.3	221.2	228.1
G	131.0	135.1	138.1	141.4	144.1	147.0	150.0	152.9
B/G	1.35	1.37	1.39	1.41	1.43	1.45	1.47	1.49
E	315.6	326.1	334.4	343.3	350.9	358.9	367.1	374.9
σ	0.204	0.207	0.211	0.214	0.218	0.221	0.223	0.226
V_L	8.63	8.75	8.84	8.93	9.01	9.09	9.17	9.24
V_S	5.26	5.32	5.35	5.39	5.41	5.44	5.47	5.50
Θ_E	898	911	920	929	937	945	954	962
A	0.443	0.449	0.449	0.452	0.451	0.452	0.454	0.456

In Tab. 3, we also list the bulk modulus and shear modulus, which can easily describe the hardness of a crystal in an indirect way. It is found that both bulk modulus B and shear modulus G increase gradually with the increasing pressure. This implies that the compressibility of LaB_6 becomes lower as the pressure increases. From the ratio of B/G, one can distinguish the ductility and brittleness of metals. The threshold is around 1.75[38]. When $B/G>1.75$, the material behaves in a ductile manner, otherwise the material behaves in a brittle manner. Duan *et al.*[14] obtained the B/G is 1.33 at 0 GPa and 0 K. The B/G as a function of pressure is displayed in Tab. 3. It can be seen that the value of B/G increases with the increasing pressure, indicating that it becomes much harder with the increasing pressure, and it is brittle in nature up to 14 GPa.

Young's modulus is defined as the ratio of stress to stain, and is used to provide a measure of the stiffness of the solid, *i. e.* the larger the value of E, the stiffer the material. Tab. 3 illustrates that Young's modulus increases with pressure when $p<14$ GPa, indicating that the pressure can, to some extent, improve the stiffness of this material. Poisson's ratio is defined as the absolute value of ratio of transverse strain to longitudinal strain, when materials subject to longitudinal stress. Poisson's ratio $\sigma=0.25$ is the lower limit for central force solids and 0.5 is the upper limit. The previous work obtained the Poisson ratio is 0.19 at 0 GPa and 0 K[14], which is in a-

greement with our work. Tab. 3 shows us that the Poisson's ratio of LaB_6 increases from 0.204 to 0.226 with the pressure up to 14 GPa. This means the interatomic forces in LaB_6 is now-central forces.

According to the elastic constants obtained, we can also obtain the compressional and shear wave velocities of LaB_6 under pressure. We list them in Tab. 3, and the results of them are V_L = 8.63 km/s and V_S = 5.26 km/s at 0 GPa, which is also in agreement with previous study (V_L = 8.625 km/s and V_S = 5.306 km/s at 0 GPa, 0 K)[14]. It is shown that in Fig. 3 that with the increasing pressure, the shear wave velocities increase. The compressional wave velocities change slowly with the elevated pressure. Unfortunately, there are no experimental data or theoretical date to be compared with our results.

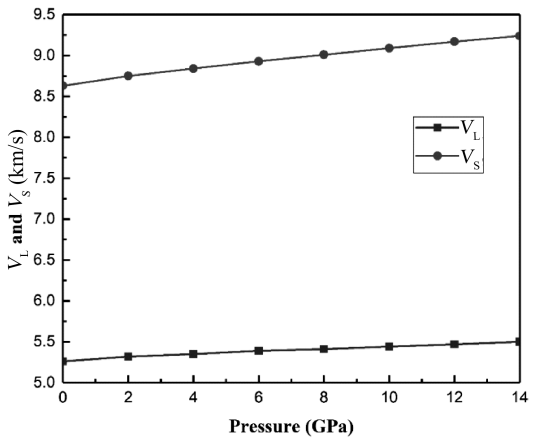

Fig. 3　The compressional and shear wave velocities of LaB_6 as a function of pressure at T=0 K

As is known, the Debye temperature is an important fundamental parameter and closely related to many physical properties of solids, such as the specific heat and melting temperature. From the elastic constants, one can obtain the elastic Debye temperature Θ_E[25, 26]. The obtained elastic Debye temperatures of LaB_6 under pressure are also presented in Tab. 3. For LaB_6 at 0 K and 0 GPa, we yield 898 K from the elastic constants of GGA calculations, which has discrepancy comparing with 1165 K obtained through quasi-harmonic Debye model at 0 K and 0 GPa by Xu *et al.*[10], but is consistent with the experiment value 878 K through ultrasonics and XRD at room temperature by Petropoulos *et al.*[39]. Obviously, the Debye temperature increases monotonically with increasing pressure up to 14 GPa.

3.3　Thermodynamic properties

The thermal expansion coefficient and specific heats C_v are the important reference to predict material properties, especially for the thermodynamic properties. We present the variations of the thermal expansion α and specific heats C_v with temperature and pressure in Figs. 4 and 5 respectively. Our calculated value for α is equal to 2.14×10^{-5} K^{-1} at 300 K, which is in agreement with the value obtained by Chen *et al.* ($\alpha = 2.10 \times 10^{-5}$ K^{-1} at 298 K)[34] and Xu *et al.* ($\alpha = 2.11 \times 10^{-5}$ K^{-1} at 298 K)[10]. Seen from the Fig. 4, at a given pressure, α increases exponentially at low temperatures and gradually approaches a linear increase at high temperatures. As the pressure increases, the growth trend of α with temperature becomes smaller and smaller, especially at high temperatures. However, at a given temperature, α decreases drastically with the increasing pressure. When the pressure increases to above 10 GPa, the thermal expansion α of 900 K is just a little larger than that of 600 K, and the curves of 600, 900, and 1200 K seem to be consistent at high pressure, which means that the temperature dependence of α is very small at high pressures and high temperatures.

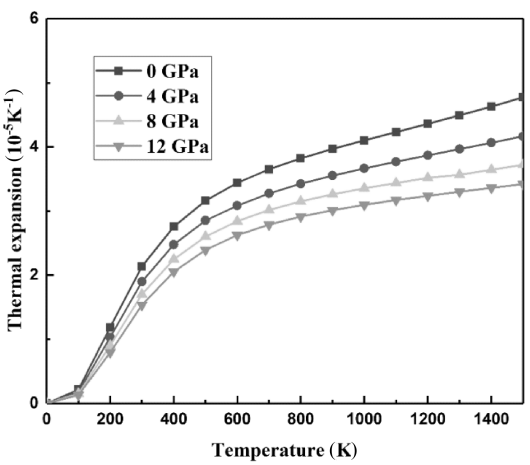

(a)

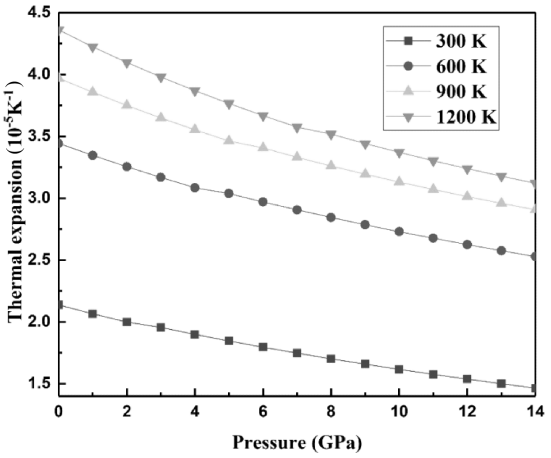

(b)

Fig. 4 Thermal expansion versus temperature and pressure of LaB_6

In Fig. 5, we can find that the C_v rise rapidly with the temperature at low temperatures, but at high temperatures, the anharmonic effect on C_v is suppressed, C_v converges slowly to the Dulong-Petit limit, about 173 J·mol^{-1}·K^{-1}, is consistent with the theoretical value 175 J·mol^{-1}·K^{-1} by Xu *et al*.[10] It also shows that the effect of temperature on the special heat capacity C_v is much larger than that of pressure.

In Fig. 6, we plotted the temperature dependence of the Debye temperature. It is well known that the Debye temperature is proportional to the bulk modulus and that hard materials exhibit elevated Debye temperatures. Our calculated Debye temperature Θ_D equals 1100 K at 300 K, in good agreement with the Θ_D calculated by Xu et al. (Θ_D=1161.5 K at 300 K)[10]. From Fig. 6, it is clearly that when T<200 K, Θ_D remains nearly constant. And then, Θ_D decreases as the temperature increases, when T>400 K, the variation of Θ_D with temperature is almost linearly increased. We can find the Debye temperature keeps above 1010 K when the temperature is up to 1500 K, which means that the effect of temperature on Debye temperature is moderate. We note the difference between the elastic Debye temperature Θ_E calculated by elastic constants (in Tab. 3) and the Debye temperature Θ_D estimated by thermodynamic methods. The elastic Debye temperature Θ_E and the Debye temperature Θ_D are 898 and 1110 K at 0 K and 0 GPa. This difference also appears in some other materials[1, 40]. This is partially because the Debye temperature Θ_D is obtained under the assumption that the material is isotropic, but LaB_6 is anisotropic. These results are consistent with the elastic anisotropic parameter A.

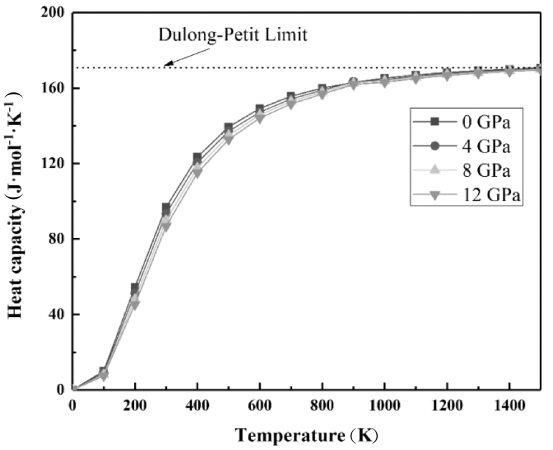

(a)

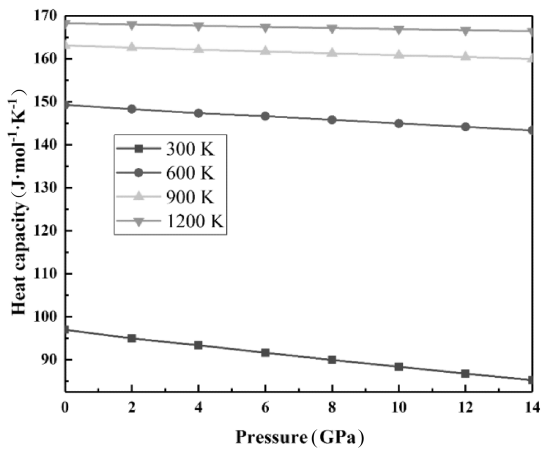

(b)

Fig. 5 The heat capacity C_v of LaB_6 as a function of temperature T at several pressures

3.4 Electronic structure

The density of states (DOS) plays an important role in the analysis of the physical properties of materials. The calculated partial density of states (PDOS) for LaB_6 is shown in Fig. 7. Our calculations at 0 GPa are consonant with the results obtained by Hossian *et al*.[13]. It is clear from the figure that the valence band can be divided into two parts. The isolated part is around

−15.0 eV with a narrow width, which arises mainly from an equal contribution of both B 2s and 2p states. The main part of valence band has a width of about 9 eV, and consists mainly of the B sp states and slightly of the La d state which is completely occupied and a small contribution of the La 6s states. It can be divided into two parts, the first part is located in the range of −11 to −7.5 eV (part Ⅰ); the second one is between −7.5 and −1 eV (part Ⅱ), and the bands located at around −10 and −5 eV have a remarkably localized characteristic. The part Ⅰ originates from almost equal contributions of B 2s and 2p orbitals, while the part Ⅱ is dominated by the B 2p orbital weekly hybridized with La 5d orbitals. Around the Fermi level, it is clearly that the B 2p state shows a strong hybridization with the La 5d states. Similarly, the conduction band can be divided into two parts depending on the weight of the PDOS, the first part is located in the range of 1 to 6 eV (part Ⅲ); the second one is between 6 and 11 eV (part Ⅳ). In part Ⅲ, the band has a remarkably localized characteristic at 3 eV and it is dominated by La 5d hybridized with the B 2sp states. While the part Ⅳ is populated with all the states of both B and La atoms.

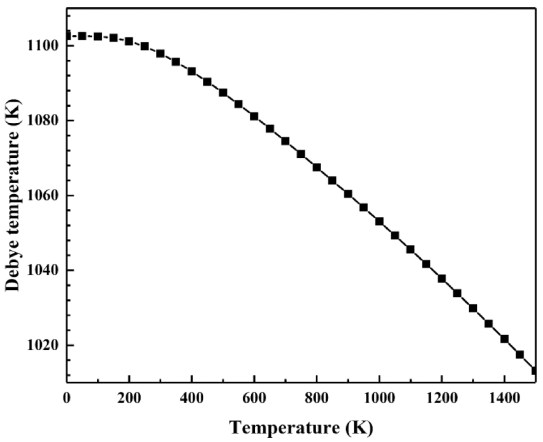

Fig. 6　Debye temperature versus temperature for LaB_6 at zero pressure

The calculated total density of states (TDOS) and partial density of states (PDOS) at high pressure (14 GPa) are also illustrated in Fig. 7. It is found that: (1) the TDOS values become larger at the sharp −5 eV when the pressure is increased, as well as the peak value of B−2s, thus, we can predict that the obtained peak is due to 2s of B; (2) all the DOS peak moves left slowly.

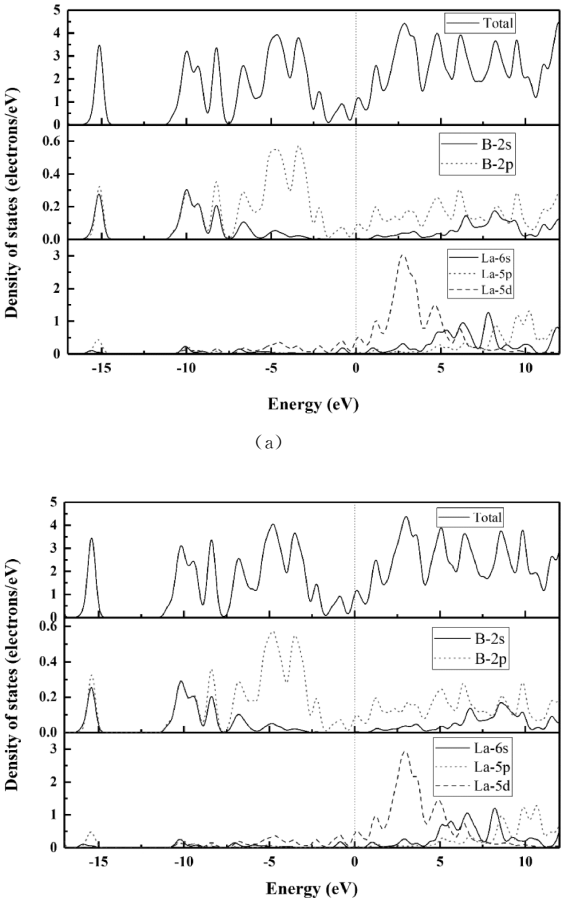

Fig. 7　Calculated total and partial density of states of structure LaB_6 at 0 GPa (a) and 14 GPa (b)

4　Conclusions

We have investigated the electronic structure and elastic properties of LaB_6 under pressure in the frame of the density functional theory. The calculated lattice parameters of LaB_6 at zero pressure and zero temperature from GGA are in agreement with the available experimental and theoretical data. The pressure dependences of elastic parameters (including elastic constants, bulk modulus, shear modulus, Young's modulus and Poisson's ratio) are also obtained. We have found that they all increase linearly with the increasing pressure. With these elastic parameters, we have studied the mechanical properties of LaB_6 under

pressure, and predicted that they are stable under pressure up to 14 GPa. We also have investigated the thermal properties of LaB_6 by utilizing quasi-harmonic Debye model. The thermal calculations show that the thermal expansion coefficient is positively related to the temperature, and negatively related to the pressure. And the effect of temperature on the special heat capacity C_v is much larger than that of pressure. Finally, we investigate the variety of the total density of states and the partial density of states of LaB_6 at diverse pressures.

References:

[1] Tang M, Liu L, Cheng Y, *et al*. First-principles study of structural, elastic, and electronic properties of CeB_6 under pressure [J]. Front Phys, 2015, 10: 107104.

[2] Zhang X, Butch N P, Syers P, *et al*. Hybridization, inter-ion correlation, and surface states in the Kondo insulator SmB_6 [J]. Phys Rev X, 2013, 3: 011011.

[3] Guy C N, Von Molnar S, Etourneau J, *et al*. Charge transport and pressure dependence of *T*c of single crystal, ferromagnetic EuB_6 [J]. Solid State Commun, 1980, 33: 1055.

[4] Kauer E. Optical and electrical properties of LaB_6 [J]. Phys Lett, 1963, 7: 171.

[5] Vandenberg J M, Matthias B T, Corenzwit E, *et al*. Superconductivity of some binary and ternary transition-metal borides [J]. Mater Res Bull, 1975, 10: 889.

[6] Tanaka T, Yoshimoto J, Ishii M, *et al*. Elastic constants of LaB_6 at room temperature [J]. Solid State Commun, 1977, 22: 203.

[7] Otani S, Ishizawa Y. Single crystals of carbides and borides as electron emitters [J]. Prog Cryst Growth Charact Mater, 1992, 23: 153.

[8] Kubo Y, Asano S. Electronic structure and positron annihilation in LaB_6 and CeB_6 [J]. Phys Rev B, 1989, 39: 8822.

[9] Mandrus D, Sales B C, Jin R. Localized vibrational mode analysis of the resistivity and specific heat of LaB_6 [J]. Phys Rev B, 2001, 64: 012302.

[10] Xu G L, Chen J D, Xia Y Z, *et al*. First-principles calculations of elastic and thermal properties of lanthanum hexaboride [J]. Chin Phys Lett, 2009, 26: 056201.

[11] Bai L, Ma N, Liu F. Structure and chemical bond characteristics of LaB_6 [J]. Physica B, 2009, 404: 4086.

[12] Gürel T, Eryiğit R. Ab initio lattice dynamics and thermodynamics of rare-earth hexaborides LaB_6 and CeB_6 [J]. Phys Rev B, 2010, 82: 104302.

[13] Hossain F M, Riley D P, Murch G E. Ab initiocalculations of the electronic structure and bonding characteristics of LaB_6 [J]. Phys Rev B, 2005, 72: 235101.

[14] Duan J, Zhou T, Zhang L, *et al*. Elastic properties and electronic structures of lanthanide hexaborides [J]. Chin Phys B, 2015, 24: 096201.

[15] Teredesai P, Muthu D V S, Chandrabhas N, *et al*. High pressure phase transition in metallic LaB_6: Raman and X-ray diffraction studies [J]. Solid State Commun, 2004, 129: 791.

[16] Godwal B K, Petruska E A, Speziale S, *et al*. High-pressure Raman and X-ray diffraction studies on LaB_6 [J]. Phys Rev B, 2009, 80: 172104.

[17] Payne M C, Teter M P, Allan D C, *et al*. Iterative minimization techniques forab initiototal-energy calculations: molecular dynamics and conjugate gradients [J]. Rev Mod Phys, 1992, 64: 1045.

[18] Clark S J, Segall M D, Pickard C J, *et al*. First principles methods using CASTEP [J]. Z Kristallogr, 2005, 220: 567.

[19] Perdew J P, Ruzsinszky A, Csonka G I, *et al*. Restoring the density-gradient expansion for exchange in solids and surfaces [J]. Phys Rev Lett, 2008, 100: 136406.

[20] Vosko S H, Wilk L, Nusair M. Accurate spin-dependent electron liquid correlation energies for local spin density calculations: a critical analysis [J]. Can J Phys, 1980, 58: 1200.

[21] Monkhorst H J, Pack J D. Special points for Brillouin-zone integrations [J]. Phys Rev B, 1976, 13: 5188.

[22] Karki B, Ackland G, Crain J. Elastic instabilities in crystals from ab initio stress-strain relations [J]. J Phys: Condens Matter, 1997, 9: 8579.

[23] Wu Z J, Zhao E J, Xiang H P, *et al*. Crystal structures and elastic properties of superhard IrN_2 and IrN_3 from first principles [J]. Phys Rev B, 2007, 76: 054115.

[24] Screiber E, Anderson O L, Soga N. Elastic constants and their measurements [M]. New York:

McGraw-Hill Book Company, 1973.

[25] Anderson O L. A simplified method for calculating the debye temperature from elastic constants [J]. J Phys Chem Solids, 1963, 24: 909.

[26] Hill R. The elastic behaviour of a crystalline aggregate [J]. Proc Phys Soc A, 1952, 65: 349.

[27] Blanco M A, Francisco E, Luana V. GIBBS: isothermal-isobaric thermodynamics of solids from energy curves using a quasi-harmonic Debye model [J]. Comput Phys Commun, 2004, 158: 57.

[28] Chen X R, Zeng Z Y, Liu Z L, *et al*. Elastic anisotropy of ε-Fe under conditions at the Earth's inner core [J]. Phys Rev B, 2011, 83: 132102.

[29] Lv Z L, Cheng Y, Chen X R, *et al*. Electronic, elastic and thermal properties of $SrCu_2As_2$ via first principles calculation [J]. J Alloys Compd, 2013, 570: 156.

[30] Zhang T, Lv Z L, Cheng Y, *et al*. Elastic and electronic properties of $MnTi_2O_4$ under pressure: a first-principle study [J]. Comput Mater Sci, 2014, 84: 156.

[31] Lu Q, Zhang H Y, Cheng Y, *et al*. Phase transition, elastic and electronic properties of topological insulator Sb_2Te_3 under pressure: first principle study [J]. Chin Phys B, 2016, 25: 026401.

[32] Ao T G, Ying C, Zhao E J, *et al*. First principles studies on mechanical Properties of ZrB_3 and NbB_2 under high Pressure [J]. J Sichuan Uni: Nat Sci Ed (四川大学学报：自然科学版), 2017, 54: 547.

[33] Birch F. Finite elastic strain of cubic crystals [J]. Phys Rev, 1947, 71: 809.

[34] Chen C H, Aizawa T, Iyi N, *et al*. Structural refinement and thermal expansion of hexaborides [J]. J Alloys Compd, 2004, 366: L6.

[35] Torsten L, Bertil L, Bert T, *et al*. An investigation of the compressibility of LaB_6 and EuB_6 using a high pressure X-ray power diffraction technique [J]. Phys Scr, 1982, 26: 414.

[36] Baranovskiy A E, Grechnev G E, Fil V D, *et al*. Electronic structure, bulk and magnetic properties of MB_6 and MB_{12} borides [J]. J Alloys Compd, 2007, 442: 228.

[37] Sin'ko G V, Smirnov N A. Ab initio calculations of elastic constants and thermodynamic properties of bcc, fcc, and hcp Al crystals under pressure [J]. J Phys: Condens Matter, 2002, 14: 6989.

[38] Pugh S F. XCII. Relations between the elastic moduli and the plastic properties of polycrystalline pure metals [J]. Philos Mag, 1954, 45: 823.

[39] Lemis-Petropoulos P, Kapaklis V, Peikrishvili A B, *et al*. Characterization of B_4C and LaB_6 by ultrasonics and X-rays diffraction [J]. Int J Mod Phys B, 2003, 17: 2781.

[40] Wei Y K, Yu J X, Li Z G, *et al*. Elastic and thermodynamic properties of CaB_6 under pressure from first principles [J]. Physica B, 2011, 406: 4476.